AIP | Applied Physics Letters

Lab-on-a-chip flow cytometer employing color-space-time coding

Sung Hwan Cho, Wen Qiao, Frank S. Tsai, Kenichi Yamashita, and Yu-Hwa Lo

Citation: Appl. Phys. Lett. **97**, 093704 (2010); doi: 10.1063/1.3481695
View online: http://dx.doi.org/10.1063/1.3481695
View Table of Contents: http://apl.aip.org/resource/1/APPLAB/v97/i9
Published by the American Institute of Physics.

Lab-on-a-chip flow cytometer employing color-space-time coding

Sung Hwan Cho,[1,a] Wen Qiao,[2] Frank S. Tsai,[2] Kenichi Yamashita,[3] and Yu-Hwa Lo[1,2]
[1]*Materials Science and Engineering Program, University of California at San Diego, La Jolla, California 92093–0418, USA*
[2]*Department of Electrical and Computer Engineering, University of California at San Diego, La Jolla, California 92093–0407, USA*
[3]*National Institute of Advanced Industrial Science and Technology (AIST), 807–1, Saga 841–0052, Japan*

(Received 5 July 2010; accepted 2 August 2010; published online 2 September 2010)

We describe a fluorescent detection technique for a lab-on-a-chip flow cytometer. Fluorescent emission is encoded into a time-dependent signal as a fluorescent cell or bead traverses a waveguide array with integrated spatial filters and color filters. Different from conventional colored filters with well-defined transmission spectral window, the integrated color filters are designed to have broad transmission characteristics, similar to the red-green-blue photoreceptors in the retina of human eye. This unique design allows us to detect multiple fluorescent colors with only three color filters based on the technique of color-space-time coding using only one single photomultiplier tube or avalanche photodetector. © *2010 American Institute of Physics*. [doi:10.1063/1.3481695]

A flow cytometer is an extensively used bioanalysis tool in medical research and clinical diagnostics to study physical and chemical properties of cells or other biological samples. Flow cytometers incorporate fluorescent detection for a greater ability to obtain detailed identification of cell types and functions based on fluorescence of antibody-conjugated dye labels. The most advanced systems can measure as many as seventeen fluorescent colors. Such multicolor detection systems find applications in immunophenotyping and stem cell research.[1–3] In spite of the valuable information obtained from the multicolor flow cytometers, the detection of multiple fluorescent colors requires many dichroic filters and photomultiplier tubes (PMTs) in order to isolate the spectral region of interest. This is the key reason why today's bench-top flow cytometers are still bulky, costly, and not easy to operate, thus having only limited use for point-of-care applications.

Lab-on-a-chip platform flow cytometers, on the other hand, are promising for point-of-care applications because they are potentially much cheaper and easier to use than bench-top systems. There have been extensive efforts to develop lab-on-a-chip platform flow cytometers.[4–8] However, although most microfluidic flow cytometer systems integrate fluidic parts and, to a very limited extent, some optical components on a single chip, they still need expensive and bulky peripheral optic and detection devices such as multiple dichroic filters and PMTs for fluorescence light detection. Concerning flow cytometers, the lab-on-a-chip approach is not attractive unless there is a significant reduction in cost and size of the system, which means the bulk optics and, in particular, the number of PMTs are reduced significantly. Since all current flow cytometers, being bench-top systems or lab-on-a-chip systems, require one dedicated PMT for detection of each fluorescence color, it calls for an innovative architecture, besides device technologies, to fundamentally alter the scaling rule (i.e., the number of optical components and PMTs does not scale linearly with the number of detection parameters).

To solve the above problem, we invent a fluorescent color detection method, color-space-time (COST) coding, for lab-on-a-chip flow cytometer applications. This is an expansion of the "space-time" coding technique we published previously that converts the spatial information into time-domain signals.[8,9] In this work, a fluorescence emission signal is encoded into a time-dependent signal when each fluorescent object passes by an array of on-chip transverse spatial filters and color filter waveguides. The on-chip spatial filters in the form of an array of apertures are made of black polydimethylsiloxane (PDMS) (Sylgard 170, Dow Corning). These spatial filters produce a specific signal waveform in time domain as illustrated schematically in Fig. 1. To add fluorescent color signals into the waveform, three waveguides each filled up with color-specific light absorption material are introduced so that the intensity of the last three peaks of the signal contain information about the fluorescent color. To separate color information from the overall fluorescence intensity of each fluorescent particle, the three leading peaks of the signal are produced from an all-pass waveguide and used as the reference intensity for each fluo-

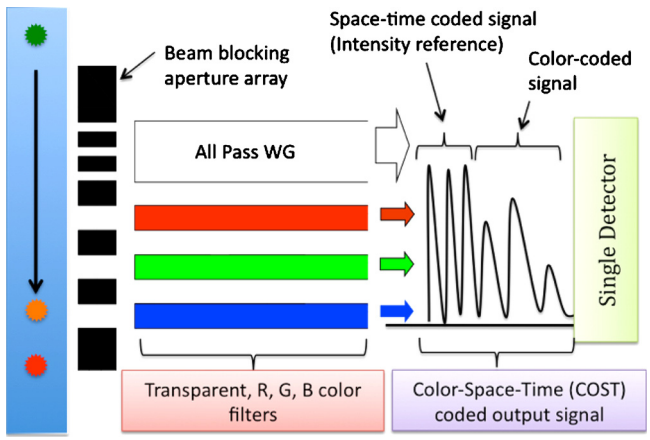

FIG. 1. (Color online) Schematic illustration of COST coding design. Each fluorescent color is first space-time coded by the first transparent waveguide, and then, color-coded by the red, green, and blue color filter waveguide array. The COST coded signal is registered by one single PMT.

[a]Electronic mail: scho@logroup.ucsd.edu.

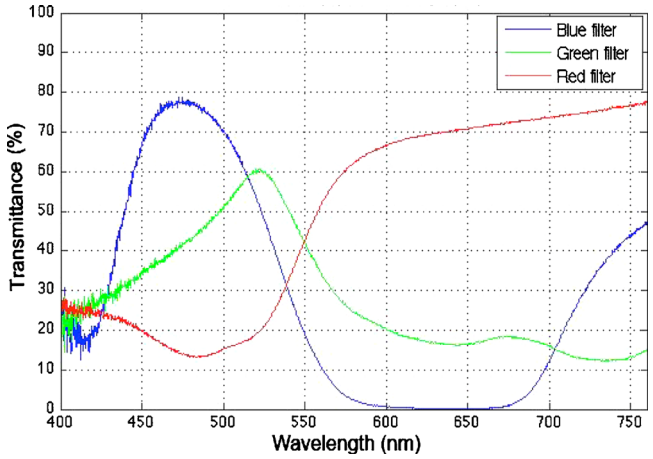

FIG. 2. (Color online) Transmission characteristics (from 400 nm to 750 nm) of red, green, and blue color filters. Each waveguide is 1 cm long. Broad transmittance spectrum filters with different peaks allow multicolor discrimination analogous to the human eye. Red filter: food color orange (300 μg/ml), green filter: phthalocyanine blue (200 μg/ml), and blue filter: food color blue (600 μg/ml).

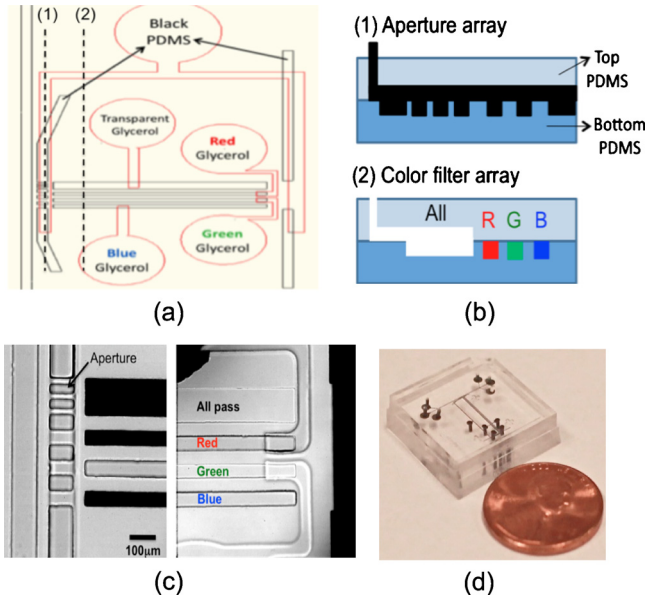

FIG. 3. (Color online) The layout of the microfluidic COST device. (a) The black patterns are for the main channels, the apertures, and the color filter waveguides. The red patterns are channels used to fill the apertures and color filter waveguides. (b) Side view of the device across lines (1) and (2) of Fig. 3(a). (c) The top and bottom PDMS layers are aligned and the waveguides and aperture are filled (d) The picture of the completed COST device.

rescent particle. A single detector (i.e., PMT) then registers the COST-coded signal, as illustrated in Fig. 1.

A COST device that provides multicolor detection on a lab-on-a-chip platform is fabricated using PDMS and glycerol. Glycerol is a good material for the waveguide core because it is optically transparent and has a higher refractive index (n=1.47) than that of PDMS (n=1.41) as the waveguide cladding material. We inject oil-soluble color dyes mixed with high refractive index glycerol into the core of on-chip waveguides as color filters to code each fluorescent color. It has been demonstrated that color dyes mixed with glycerol do not diffuse into the PDMS cladding layers, thus resulting in stable color filter waveguides.[10] Orange food color powders (AmeriColor Co.), phthalocyanine blue dyes (TCI Chemicals, Inc.) and blue food color powders (AmeriColor Co.) are chosen to form the red, green, and blue color filter waveguides, respectively. After calibrating the concentration of each color filter in glycerol, we achieve the desired transmission spectrum of each waveguide filter as shown in Fig. 2.

To distinguish as many fluorescent colors as possible, we have each color [red-green-blue (RGB)] waveguide show a gradual change in its transmission spectrum in a similar manner to the photoreceptors found in the combs of human retina.[11] The gradual, wideband color filtering reduces the required number of samples to differentiate multiple colors, and its principle has been manifested by our eye's ability to distinguish more than 1000 colors using only three kinds of photoreceptors. For lab-on-a-chip flow cytometers, we attempt to use three on-chip color-filtered waveguides to detect as many as 11 wavelengths using a single PMT.

The microfluidic COST device is fabricated by PDMS replica molding process using an SU-8 mold formed photolithographically on a silicon wafer. The device contains several structures including (i) microfluidic channels, (ii) apertures and color filter waveguides, and (iii) another channel structure for filling the apertures and the waveguide channels. Patterns in [(i) and (ii)] and in (iii) are formed on two separate PDMS substrates first and then the two PDMS substrates are UV/O-zone bonded together with an alignment accuracy better than 10 μm.

Figure 3(a) shows the layout of the device consisting of two (black and red) layers of patterned PDMS that are bonded together. The black patterns in Fig. 3(a) are the main channels, the apertures, and the color filter waveguides. The red patterns are channels for fluids filling to create the apertures and the color filter waveguides. Figure 3(b) shows the side view of the device across lines (1) and (2) of Fig. 3(a). Figure 3(c) shows well aligned top and bottom PDMS layers. The apertures for space-time coding and for stray light blocking are filled with black PDMS by the capillary effect. After 30 min of curing, the all-pass (i.e., dye-free) and RGB color filter waveguide channels are filled with appropriately doped glycerol by the capillary effect as well. All the waveguides are filled without any air bubbles.

Using the COST device, we demonstrate that two fluorescent microbeads emitting two different, although similar, colors can be distinguished using a single PMT (PMM02, Thorlabs Inc.). A 488 nm wavelength diode laser (40 mW, Coherent) is used as the source to excite the beads in the microfluidic channel. The spot of the excitation laser has a Gaussian intensity profile and the laser intensity across the 450 μm waveguide regime is calibrated using a charge-coupled device camera. In the final data analysis for color discrimination, the effect of laser intensity distribution is removed.

Figure 4(a) shows a typical waveform of the COST coded output signal from a dragon green fluorescent bead. The emission peak is at 520 nm, equivalent to fluorescein isothiocyanate fluorochrome that is widely used in flow cytometers. The first three peaks are space-time coded signals. They establish the reference for the overall fluorescence intensity so that the fluorescence intensity variations among different beads will not affect our ability to determine the fluorescent colors. The last three peaks have different intensities because each peak is produced by the corresponding

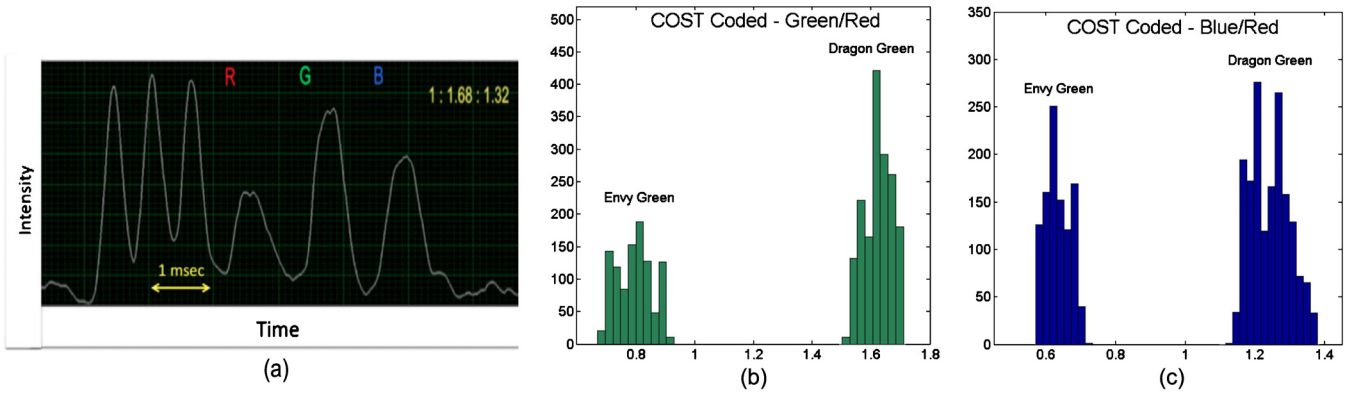

FIG. 4. (Color online) (a) COST modulated signal of Dragon Green fluorescence. The first three lobes are space-time coded signals, and the following three peaks are the COST coded signal. (b) Histogram of the green filtered COST-coded signal normalized to the red filtered signal intensity of Dragon green and Envy green. (c) Histogram of the blue filtered COST-coded signal of Dragon green and Envy green.

color filter based on the overlap between the emission spectrum of each type of fluorophore and the transmission spectrum of the color filter. In consequence, the intensity ratios among these three peaks produce a unique fingerprint for each type of fluorophore. Figure 4(b) shows the histogram of the green filtered COST-coded signal of the dragon green and the envy green (emission peak at 565 nm) fluorescent colors, which is normalized to the red filtered signal. In the same way, the histogram of the blue-filtered COST-coded signal of the two fluorescent colors is shown in Fig. 4(c).

Dragon green is represented by a vector [1, 1.63 (σ =0.046), 1.24 (σ=0.055)] while envy green is represented by a vector [1, 0.80 (σ=0.060), 0.64 (σ=0.034)]. The variations (e.g. standard deviation) for each "color fingerprint" are between 2% and 7%.

Likewise, more fluorescent colors can be represented by their unique fingerprints according to the intensity ratios of (green/red, blue/red). The overlap between the emission spectrum of each fluorophore and the transmission spectrum of the RGB color filters in Fig. 2 determines the center position of each fluorophore in Fig. 5. The ellipse around each color represents the boundary of 5% fluctuation of the color ratios. From the data in Fig. 5, we conclude that 11 different commonly used fluorophores in flow cytometers can be detected with a single PMT using the COST technique. Ultimately the number of colors that can be detected with the COST technology will be limited by the electronic noise.

Fingerprints of 11 fluorochromes		
	Green/Red	Blue/Red
Cascade Yellow	0.906	0.509
Pacific Blue	1.751	2.463
Pacific Orange	0.796	0.385
Alexa488	1.594	1.063
PerCP	0.580	0.330
R-PE	0.672	0.115
Cy5	0.446	0.179
Cy5-5	0.401	0.388
Cy7	0.292	0.696
QD 545	1.199	0.715
QD 565	0.706	0.250

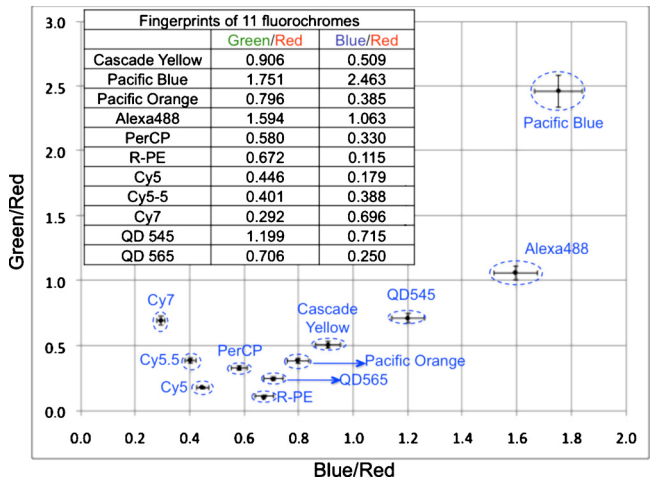

FIG. 5. (Color online) Each fluorescent color in the table has its fingerprint presented by the blue/red and green/red intensity ratios. The ellipse around each center position is the boundary of 5% fluctuation in the intensity ratios. The figure shows 11 commonly used fluorophores in flow cytometers can be distinguished with a single PMT using the COST technique.

In conclusion, we have fabricated a lab-on-a-chip flow cytometer that has a unique architecture to support the COST coding technique. Using the COST technique, beads of two different fluorescent colors can be distinguished using a single PMT. The architecture is highly scalable and we have shown that as many as 11 commonly used fluorophores in flow cytometers can be detected with a single PMT (or APD). Since bulk optics and a large number of PMTs are the bottleneck for the cost and size reduction in today's flow cytometers and the key reasons for system failures and high maintenance, the lab-on-a-chip technology in conjunction with the COST technique holds great promise for compact, cost effective, and easy to use flow cytometers for point-of-care applications.

The authors acknowledge the technical support of the staff of the UCSD Nano3 (Nanoscience, Nanoengineering, and Nanomedicine) facility in Calit2. We also thank Jason Karp for loaning us a long working microscope objective lens. The work is supported by NIH Grant Nos. R01HG004876 and R21RR024453.

[1]P. Chattopadhyay, D. A. Price, T. H. Harper, M. R. Betts, J. Yu, E. Gostick, S. P. Perfetto, P. Goepfert, R. A. Koup, S. C. D. Rosa, M. P. Bruchez, and M. Roederer, Nat. Med. **12**, 972 (2006).
[2]N. Baumgarth and M. Roederer, J. Immunol. Methods **243**, 77 (2000).
[3]S. De Rosa, L. Herzenberg, L. Herzenberg, and M. Roederer, Nat. Med. **7**, 245 (2001).
[4]J. Godin, V. Lien, and Y.-H. Lo, Appl. Phys. Lett. **89**, 061106 (2006).
[5]M. McClain, C. Culbertson, and S. Jacobson, Anal. Chem. **73**, 5334 (2001).
[6]Z. Wang, J. El-Ali, M. Engelund, T. Gotsaed, I. R. Perch-Nielsen, K. B. Mogensen, D. Snakenborg, J. P. Kutter, and A. Wolff, Lab Chip **4**, 372 (2004).
[7]J. Kruger, K. Singh, A. O'Neill, C. Jackson, A. Morrison, and P. O'Brien, J. Micromech. Microeng. **12**, 486 (2002).
[8]S. H. Cho, C. H. Chen, F. S. Tsai, J. M. Godin, and Y.-H. Lo, Lab Chip **10**, 1567 (2010).
[9]C. H. Chen, S. H. Cho, F. S. Tsai, A. Erten, and Y.-H. Lo, Biomed. Microdevices **11**, 1223 (2009).
[10]C. L. Bliss, J. N. McMullin, and C. J. Backhouse, Lab Chip **8**, 143 (2008).
[11]M. F. Land and D. E. Nilsson, *Animal Eyes* (Oxford University Press, New York, 2002).